Amplification Factor of Echo Signals in Ferrimagnetic Materials

Hoton How, Carmine Vittoria, *Fellow, IEEE*, and Glen E. Everett, *Associate Member, IEEE*

Abstract—**It is well known that spin echoes in ferrimagnetic materials can only be excited upon the application of high power microwave signals. In this paper the amplification factor of spin echoes is calculated for ferrimagnetic materials in which long-range dipolar fields, external rf-field couplings, and magnetization relaxations are included in the calculations. The inclusion of such interactions provide a mechanism by which realistic amplification of echoes may be calculable. Our theoretical estimate of amplification is in reasonable agreement with previous experiments. We have, thus, systematically calculated the effects of carrier frequency, field gradient, and microwave power upon echo amplification.**

Introduction

ECHO phenomena is characterized by the re-radiation of the input signals stored in a nonlinear system through the agitation of a consequently applied pump pulse. Observation of ferrimagnetic echoes was first reported in 1965 by Kaplan [1] in polycrystalline yttrium iron garnet (YIG) samples. Amplified echoes were thereafter reported in cylinders and truncated spheres of YIG crystals [2]–[5], and in single crystal YIG films [6], [7]. Echo experiments offer the possibility of a novel approach to performing important signal processing functions, such as nondispersive time delay and pulse correlation in the frequency range below 10 GHz [8]. Within the demand of electronic technology advances there is also a renewed interest toward the use of Ferrimagnetic Echo Devices (AFED's). Earlier theoretical work was successful in arguing for the presence of ferrimagnetic echoes and possibilities for amplification [9], [10]. However, quantitative predictions of the amplification factor either ranged several orders of magnitude greater than observed [9] or even unyielding [10]. Previous theoretical formulations were derived in terms of a nonlinear equation of motion in which the nonlinearity was introduced ad hoc by raising the instantaneous magnetization to the third power. The nonlinear term was not identified in terms of any source of internal fields. The linearized terms included the external magnetic field, its gradient, and exchange field. This type of formulation predicted undamped magnetization amplitude even long after the removal of the excitation pulses, and it gave rise to amplified echoes only at extraordinarily long delay times at which the exchange field becomes appreciable. This result was unrealistic, since at such long delay times the ordinary magnetization relaxation field, which was ignored in the theory, will eventually damp out the occurrence of any echo.

The purpose of this paper is to precisely formulate the equation of motion governing the "growth" of echoes in ferrimagnetic materials and calculate realistic amplification factor of echoes. The theory includes treatment of conventional fields, such as the external dc fields and the exchange field, as well as the non-trivial long-range dipole-dipole interaction, the Gilbert damping field, and the coupling of external rf fields. The latter three terms are introduced in the equation of motion for the first time in the analysis of echo formulation in ferrimagnetic materials. Preliminary results of our theory have been published in [11]. We find that in contrast to previous theory [10], the exchange field has very little effect in amplifying an echo. Also, the dipole-dipole nonlocal field plays a significant role in the relaxation of magnetization and, hence, the amplification factor. The cross dimensions of the sample plays an important role in the echoing process as experimentally verified in [5]. Our theory predicts an echo gain which compares reasonably well with experiments. This theory also predicts the following. For a given cross sectional dimension, L, of the sample and fixed field gradient there exists a threshold power for the pump signal above which the echo gain could be appreciably enhanced. The echo gain monotonically decreases if the carrier frequency as modulated by the pulse is increased. For a given L there exists an optimal value of the field gradient upon which the echo gain is maximized; the gain reduces to zero if the field gradient is further increased to very large values.

The paper is organized as follows. The non-local aspect of the equation of motion is developed in the formulation section. The section on results reports the effect of physical parameters on the amplification factor of the echo signals: the field gradient, the pump signal, and the carrier frequency, etc. Finally, the discussion and conclusions summarize the paper.

Manuscript received January 16, 1991; revised June 17, 1991. This work was sponsored by the U.S. Office of Naval Research (ONR).

H. How and C. Vittoria are with the Department of Electrical and Computer Engineering, Northeastern University, Boston, MA 02115,

G. E. Everett is with the Department of Physics, University of California, Riverside, CA 92521.

IEEE Log Number 9102816.

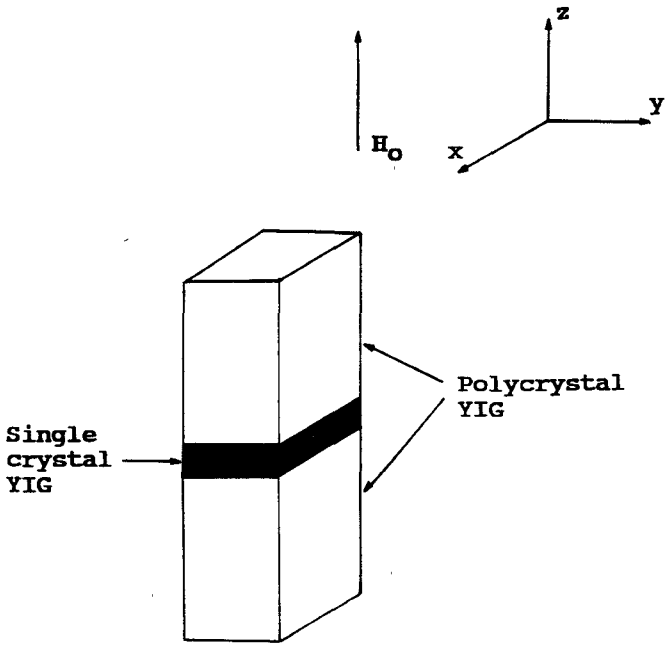

Fig. 1. Sample configuration used in the formulation.

Formulation

We consider a single crystal YIG cylinder of rectangular cross section and infinitely long. The dc field is applied along the cylindrical axis and a gradient of the field is assumed. Experimentally, this geometrical configuration is simulated by sandwiching a thin disk of YIG crystal in between two polycrystalline cylinders as shown in Fig. 1 [3]–[5]. In this configuration the carrier frequency and the dc uniform field should be carefully adjusted such that the active echoing region falls within the crystal disk. While the echo gain can be very high in this configuration, the frequency bandwidth is limited by the small thickness of the single crystal disk. However, if we switch the experimental configuration from that of a cylinder to a planar configuration in which H is in the film plane, echoes could occur over wide frequency bandwidth, but the observed echo gains were relatively low [6], [7]. For either configuration the Gilbert equation of motion may be assumed as

$$\frac{-1}{\gamma}\dot{\vec{M}} = \vec{M}\times\vec{H}_{\text{eff}} - \frac{\lambda}{\gamma^2 M_s^2}\vec{M}\times\dot{\vec{M}}, \tag{1}$$

where γ is the gyromagnetic ratio, λ the Gilbert damping constant, and $\vec{H}_{\text{eff}}$ is the effective field which includes the following:

$$\vec{H}_{\text{eff}} = (H_o + Gz - 4\pi N_z M_z)\hat{z} + \vec{h}_{ex} + \vec{h}_m + \vec{h}_s. \tag{2}$$

Here H_o is the applied magnetic field, G the constant field gradient, N_z the demagnetizing factor in the z-direction (≈ 0), $\vec{h}_{ex}$ is the exchange field given by

$$\vec{h}_{ex} = \Lambda\nabla^2\vec{M}, \tag{3}$$

and $\vec{h}_s$ is the externally applied rf field. $\vec{h}_m$ is the dipolar field associated with the transverse magnetization $\vec{m}$ as obtained from

$$\vec{\nabla}\cdot\vec{h}_m = -4\pi\vec{\nabla}\cdot\vec{m}. \tag{4a}$$

Under magnetostatic approximation $\vec{h}_m$ satisfies the condition

$$\vec{\nabla}\times\vec{h}_m = 0. \tag{4b}$$

From (4a) and (4b) $\vec{h}_m$ may be solved for a given distribution of $\vec{m}$ subject to the boundary conditions:

$$\vec{h}_m = 0 \text{ at infinity.} \tag{4c}$$

The total magnetization $\vec{M}$ is

$$\vec{M} = M_z\hat{z} + \vec{m}. \tag{5a}$$

Under sufficiently high excitation power the magnetization is driven into nonlinear regime and the longitudinal magnetization may be approximated as

$$\begin{aligned} M_z &= \left(M_s^2 - \vec{m}\cdot\vec{m}\right)^{1/2} \\ &\approx M_s - (1/2M_s)\vec{m}\cdot\vec{m}. \end{aligned} \tag{5b}$$

In (5b) we have kept the Taylor expansion up to the third order in $\vec{m}$. The transverse part of (1) can be then written as

$$\begin{aligned} \frac{-1}{\gamma}\dot{\vec{m}} = \hat{z}\times\Bigg[& -(H_o + Gz - 4\pi N_z M_s)\vec{m} \\ & + M_s\left(\vec{h}_m + \vec{h}_s + \vec{h}_{ex}\right) \\ & - \frac{1}{\gamma^2 M_s}\dot{\vec{m}} - \hat{z}\cdot\left(\vec{h}_m + \vec{h}_s + \vec{h}_{ex}\right)\vec{m} \\ & - \frac{\vec{m}\cdot\vec{m}}{2M_s}\left(\vec{h}_m + \vec{h}_s + \vec{h}_{ex} + 4\pi N_z\vec{m}\right) \\ & + \frac{\lambda}{\gamma^2 M_s^2}\left(\frac{\vec{m}\cdot\vec{m}}{2M_s}\dot{\vec{m}} - \frac{\vec{m}\cdot\dot{\vec{m}}}{M_s}\vec{m}\right)\Bigg]. \end{aligned} \tag{6}$$

The longitudinal part of (1) can be proved to be equivalent to (6). Anisotropic magnetic fields have been omitted in (6) since the dc field is applied along a cubic major axis. Also, anisotropic magnetic fields are small in YIG when compared to the demagnetizing fields. As we may see at the end of this calculation, the exchange and spin relaxation effects are not very significant under normal echoing conditions. As such, we keep only the linear terms in λ and Λ in (6), or

$$\begin{aligned} \dot{\vec{m}} = \hat{z}\times\Bigg[& (H_o + G'z)\vec{m} - \left(1 - \frac{\vec{m}\cdot\vec{m}}{2}\right)\left(\vec{h}_m + \vec{h}_s + 4\pi N_z\vec{m}\right) \\ & - \Lambda\nabla^2\vec{m} + \lambda'\dot{\vec{m}} - \hat{z}\cdot\vec{h}_m\vec{m}\Bigg], \end{aligned} \tag{7}$$

where magnetization and fields have been normalized with respect to M_s and the time has been normalized with respect to $(\gamma M_s)^{-1}$. The parameters G' and λ' in (7) are

normalized as follows:

$$G' \equiv G/4\pi M_s, \qquad \lambda' \equiv \lambda/\gamma M_s.$$

Henceforth, the prime will be dropped. In (7) we have taken $\hat{z}\cdot\vec{h}_s = 0$ by assuming $\vec{h}_s$ to be a transverse field.

From (4a) to (4c) the dipolar field $\vec{h}_m$ may be solved utilizing the Green's theory as [12]

$$\vec{h}_m = \bar{\nabla}\mathcal{G}\vec{\nabla}\cdot\vec{m}, \tag{8}$$

where the Green's function operator $\mathcal{G}$ is defined, upon operation on a regular function $f(\vec{r})$, as

$$\mathcal{G}f(\vec{r}) = \int_{\text{all space}} d\vec{r}'\cdot\frac{1}{|\vec{r}-\vec{r}'|}\cdot f(\vec{r}'). \tag{9}$$

We introduce the following definitions:

$$\partial^{\pm} \equiv \partial/\partial x \pm i\partial/\partial y,$$
$$h_o \equiv (\vec{h}_s)_x + i(\vec{h}_s)_y,$$
$$\alpha \equiv m_x + im_y.$$

Equation (7) can then be rewritten as

$$\dot{\alpha} = i\Bigg[(H_o + Gz)\alpha - \left(1-\frac{|\alpha|^2}{2}\right)\left(\frac{1}{2}\partial^+\mathcal{G}\partial^-\alpha + \frac{1}{2}\partial^+\mathcal{G}\partial^+\alpha^* + 4\pi N_z\alpha + h_o\right) - \Lambda\nabla^2\alpha + \lambda\dot{\alpha} - \alpha\frac{\partial}{\partial z}\mathcal{G}\left(\frac{1}{2}\partial^-\alpha + \frac{1}{2}\partial^+\alpha^*\right)\Bigg]. \tag{10}$$

Assume (10) possesses solution of the following form

$$\alpha(\vec{r},t) = \alpha(z,t)\cdot\sin(\pi x/a)\cdot\sin(\pi y/b) \tag{11}$$

with a and b being the planar cross dimensions of the sample. Equation (11) corresponds to solutions which minimizes the exchange energy. Under uniform rf excitations (11) represents solutions that best approach the real solutions with definite k_x and k_y values and satisfy the boundary conditions imposed at the sample surfaces. Nevertheless, it can never satisfy (10) rigorously, since the nonlinearity in (10) will couple the above solutions to higher order modes of k_x and k_y values. However, since the nonlinearity is small, we may assume (11) satisfies (10) in the sense of average, i.e., (11) is substituted in (10) which is then followed by taking average over the x and y-dimensions. This is the only approximation that we will make in this theoretical treatment. This approximation is roughly valid if the input power is not very high. Under very high power excitations energy will transfer from the lowest excitation state, (11), into higher order modes, and (11) can still be adequately used if the damping constant λ in (10) is modified by including a power dependent term:

$$\lambda \to \left[1 + O(|\alpha|^2)\right]\lambda.$$

This implies that one must retain in (6) nonlinear terms which are proportional to λ and Λ.

The formulation can be largely simplified if we adopt the following expression for the Green's function kernel:

$$\frac{1}{|\vec{r}-\vec{r}'|} = \frac{1}{2\pi^2}\int_{\text{all space}} d\vec{k}\cdot\frac{e^{i\vec{k}\cdot(\vec{r}-\vec{r}')}}{k^2}. \tag{12}$$

In this manner $\partial^+\mathcal{G}\partial^-\alpha$, for example, can be written as

$$\begin{aligned}\partial^+\mathcal{G}\partial^-\alpha &= \frac{-1}{2\pi^2}\int_{-\infty}^{\infty}\int_{-\infty}^{\infty} d\vec{r}'\,d\vec{k}\left[\partial^-\partial^+\cdot\frac{e^{i\vec{k}\cdot(\vec{r}-\vec{r}')}}{k^2}\right]\\ &\quad\cdot\alpha(z',t)\cdot\sin(\pi x'/a)\sin(\pi y'/b)\\ &= -2\left[\frac{\pi^2}{a^2}+\frac{\pi^2}{b^2}\right]\sin(\pi x/a)\sin(\pi y/b)\\ &\quad\cdot\int_{-\infty}^{\infty}\int_{-\infty}^{\infty} dz'\,dk\cdot\alpha(z',t)\frac{e^{ik(z-z')}}{\pi^2/a^2+\pi^2/b^2+k^2}\\ &= -2\pi p\cdot\sin(\pi x/a)\cdot\sin(\pi y/b)\\ &\quad\cdot\int_{-\infty}^{\infty} dz'\cdot\alpha(z',t)e^{-p|z-z'|},\end{aligned} \tag{13}$$

where p is defined as

$$p = \left[(\pi/a)^2 + (\pi/b)^2\right]^{1/2}, \tag{14}$$

and integral by parts has been used in deriving (13). Similar results can be obtained for $\partial^+\mathcal{G}\partial^+\alpha^*$, $(\partial/\partial z)\mathcal{G}\partial^-\alpha$, and $(\partial/\partial z)\mathcal{G}\partial^+\alpha'$. Average over x and y dimensions can be then readily carried out for (10). It implies

$$\dot{\alpha} = i\Bigg[(H_o + Gz + \Lambda p^2)\alpha - \Lambda\frac{\partial^2\alpha}{\partial z^2} + \lambda\dot{\alpha} - \frac{\pi^2}{4}\left(1-\frac{2}{9}|\alpha|^2\right)(h_1+h_2) - 4\pi N_z\left(1-\frac{2}{9}|\alpha^2|\right)\alpha - \frac{\pi^2}{4}\left(1-\frac{1}{8}|\alpha|^2\right)h_0\Bigg], \tag{15}$$

where h_1 and h_2 are defined as

$$h_1 \equiv \frac{-4p}{\pi}\int_{-\infty}^{\infty} dz'\cdot e^{-p|z-z'|}\cdot\alpha(z',t), \tag{16}$$

$$h_2 \equiv \frac{-4q^2}{\pi p}\int_{-\infty}^{\infty} dz'\cdot e^{-p|z-z'|}\cdot\alpha(z',t)^*, \tag{17}$$

and q is defined as

$$q = \left[(\pi/\alpha)^2 - (\pi/b)^2\right]^{1/2}. \tag{18}$$

The non-local effects are expressed in the above two fields, h_1, and h_2. In the limit that p goes to infinity the integrations in the above expressions are over narrow regions. Hence, h_1 and h_2 could only represent some sort of local field. Note that the term $\hat{z}\cdot\vec{h}_m\vec{m}$ in (7), or the last term in (10), has been averaged out in (15), since $\hat{z}\cdot\vec{h}_m$ can be expressed in terms of products involving $\cos(\pi x/a)$ or $\cos(\pi y/b)$, while $\vec{m}$, or α, is expressed in sine terms as shown in (11). Therefore, (15) contains only linear and cubic terms in α, which confirms the generally

recognized fact that the nonlinearity must be of an odd order in order to generate an echo [8].

In the following we will omit the dipolar field h_2 by assuming $a \approx b$ and hence $q \approx 0$. This corresponds to the general circular-precession approximation imposed in the normal linear-mode calculation and is equivalent to neglecting the third Holstein–Primakoff transformation for spin waves [13]. Non-circular precessional fields will have profound effect on echo amplification if the sample posseses very different cross sectional dimensions, for example, as in the film geometry. Echo amplification in the film geometry will be discussed in a future paper.

Furthermore, we notice that the nonlinear terms corresponding to the nonlocal interaction, $h_1|\alpha|^2$, and to the static-demagnetization, $\alpha|\alpha|^2$, have opposite signs in (15). This can be most readily checked via (16) when the local approximation is assumed: $p \to \infty$. Therefore, as we will see at the end of this calculation, while the former is responsible for the amplification of the echoed signal, the latter would simply reduce the gain. As it was pointed out by Suhl [14] that the static-demagnetization is closely related to the spinwave instability occurring in the subsidiary absorption at microwave resonance measurements, we find here that this nonlinearity can also have an adverse effect on achieving echo amplification and hence should be avoided. Thus it is advantageous to place discs of single crystal YIG in between polycrystalline YIG cylinders [3]–[5]. In the following calculation we will take $N_z = 0$.

Suppose the excitation circuit element provides right-hand circularly polarized pulses of the following form:

$$h_0(t) = A_o\delta(t) + \epsilon_o\delta(t+\tau), \tag{19}$$

where A_o and ϵ_o are the amplitudes of the pump and the signal pulses applied at $t = 0$ and $t = -\tau$, respectively. We assume $\epsilon_o \ll 1$. Under the above excitation solutions following (15) may be argued to have the following form:

$$\alpha(z,t) = \Psi(t)\cdot\left[A\cdot e^{iGzt} + \epsilon\cdot\psi_1(t)\cdot e^{iGz(t+\tau)} + \epsilon\cdot\psi_2(t)\cdot e^{iGz(t-\tau)}\right]. \tag{20}$$

As it will be shown later, with the above functional form of $\alpha(z,t)$ (15) becomes separable in variables z and t exactly up to first order in ϵ ($\ll 1$). Relationships between A_o and A and between ϵ_o and ϵ can be obtained by integrating (15) from $t = 0^-$ to $t = 0^+$, and from $t = -\tau^-$ to $t = -\tau^+$ as

$$|A_o| = \frac{4}{\pi^2}\frac{A}{1 - A^2/32}, \tag{21a}$$

$$|\epsilon_o| = \frac{4}{\pi^2}\epsilon. \tag{21b}$$

Consequently the inhomogeneous integral-differential equation, (15), can be converted into an initial value problem satisfying, for $t > 0$, the following equation:

$$\dot{\alpha} = i\left\{\left[(1+i\lambda)(H_o + \Lambda p^2) + Gz\right]\alpha - \Lambda\frac{\partial^2\alpha}{\partial z^2} - \frac{\pi^2}{4}h_1\left(1 + i\lambda - \frac{2}{9}|\alpha|^2\right)\right\}, \tag{22}$$

with the initial values

$$\psi(0) = 1, \tag{23a}$$

$$\psi_1(0) = 1, \tag{23b}$$

$$\psi_2(0) = 0. \tag{23c}$$

In the above we have assigned the phases of the initial values arbitrarily to zero. Note that we have assumed $\lambda \ll 1$ in writing (22). The detected output is the averaged value of h_1

$$\langle h_1\rangle = \lim_{L\to\infty}\frac{-4p}{\pi}\int_{-L}^{L}\frac{dz}{2L}\cdot\int_{-\infty}^{\infty}e^{-p|z-z'|}\cdot\alpha(z')\cdot dz' = \frac{-8}{\pi}\langle\alpha\rangle, \tag{24}$$

which provides non-vanishing values only at times $t = 0$, $\pm\tau$, see (20). The echo gain is, therefore,

$$\text{Gain} = \left|\frac{\langle h_1\rangle}{\epsilon_o}\right|_{t=\tau} = 2\pi|\psi(\tau)\cdot\psi_2(\tau)|. \tag{25}$$

The dipolar field associated with expression (20) can be written as

$$h_1(z,t) = \frac{-8p}{\pi}\Psi(t)\cdot\left[A\cdot\frac{e^{iGzt}}{p - iGt} + \epsilon\cdot\psi_1(t)\cdot\frac{e^{iGz(t+\tau)}}{p - iG(t+\tau)} + \epsilon\cdot\psi_2(t)\cdot\frac{e^{iGz(t-\tau)}}{p - iG(t-\tau)}\right]. \tag{26}$$

Before proceeding further we notice here that, since the final answer only involves the averaged value of α, (24) and (25), the linear terms in h_1 in (22) may be replaced by $(-8/\pi)\alpha$ to simplify the following calculations. Furthermore we may translate the origin of the z-coordinate such as to cancel the linear terms in α possessing pure imaginary coefficients. By doing so the effective dc-field comes out to be

$$H_{dc} = H_o + \Lambda p^2 + 2\pi, \tag{27}$$

where the last component 2π may be interpreted as the normal rf-demagnetizing effect associated with the transverse directions of the sample ($N_x = N_y = 1/2$) [15]. We introduce the parameter ν as

$$\nu = H_{\text{dc}}\cdot\lambda. \tag{28}$$

Note that H_{dc} determines the location of the active region of the sample and hence the carrier frequency of the excitation pulses. After expressions (20) and (26) have been substituted in (22), one may set the coefficients corresponding to $\exp(iGzt)$, $\exp[iGz(t+\tau)]$, and

$\exp[iGz(t-\tau)]$ separately to zero, and one obtains

$$\dot{\psi} = i\left(\Lambda G^2 t^2 + i\nu - \frac{4\pi}{9}\cdot\frac{A^2|\Psi|^2}{1-iGt/p}\right)\Psi, \tag{29a}$$

$$\dot{\psi}_1 = i\left[\left(\Lambda G^2\tau^2 + 2\Lambda G^2\tau t - \frac{4\pi}{9}\cdot\frac{A^2|\Psi|^2}{1-iG(t+\tau)/p}\right)\psi_1 - \frac{4\pi}{9}\cdot\frac{A^2|\Psi|^2}{1-iGt/p}\cdot\psi_2^*\right], \tag{29b}$$

$$\dot{\psi}_2 = i\left[\left(\Lambda G^2\tau^2 - 2\Lambda G^2\tau t - \frac{4\pi}{9}\cdot\frac{A^2|\Psi|^2}{1-iG(t-\tau)/p}\right)\psi_2 - \frac{4\pi}{9}\cdot\frac{A^2|\Psi|^2}{1-iGt/p}\cdot\psi_1^*\right]. \tag{29c}$$

We define the new variables $W(t)$, $\phi_1(t)$, and $\phi_2(t)$ as

$$W(t) \equiv |\psi(t)|\cdot\exp(\nu t), \tag{30a}$$

$$\phi_1(t) \equiv \psi_1(t)\cdot\exp(-i\Lambda G^2\tau t^2), \tag{30b}$$

$$\phi_2(t) \equiv \psi_2(t)\cdot\exp(i\Lambda G^2\tau t^2), \tag{30c}$$

and new parameters B, g, and Γ as

$$B \equiv \Lambda G^2\tau^3, \tag{31a}$$

$$g \equiv G\tau/p, \tag{31b}$$

$$\Gamma \equiv (4\pi/9)A^2\tau. \tag{31c}$$

Equations (29a) to (29c) can be then rewritten as

$$\dot{W} = \frac{-\Gamma g t e^{-2\nu\tau t}}{1+g^2t^2}W^3, \tag{32a}$$

$$\dot{\phi}_1 = i\left\{\left[B - \frac{\Gamma W^2 e^{-2\nu\tau t}}{1-ig(t+1)}\right]\phi_1 - \frac{GW^2e^{-2\nu\tau t}}{1-igt}\phi_2^*\right\}, \tag{32b}$$

$$\dot{\phi}_2 = i\left\{\left[B - \frac{\Gamma W^2 e^{-2\nu\tau t}}{1-ig(t-1)}\right]\phi_2 - \frac{GW^2e^{-2\nu\tau t}}{1-igt}\phi_1^*\right\}. \tag{32c}$$

In (32a) to (32c) the time variable has been normalized with respect to the echo delay time τ. Note that $W(t)$ is real and $\phi_1(t)$ and $\phi_2(t)$ are complex quantities, and the initial values for $W(t)$, $\phi_1(t)$, and $\phi_2(t)$ are

$$W(0) = 1, \tag{33a}$$

$$\phi_1(0) = 1, \tag{33b}$$

$$\phi_2(0) = 0. \tag{33c}$$

The echo gain can be expressed as

$$\text{Gain} = 2\pi W(1)|\phi_2(1)|\exp(-\nu\tau). \tag{34}$$

We note here that we have developed in the above a new calculation scheme in deducing the dynamical equation of motion, (32a) to (32c), from its precursory equation which is coupled nonlinearly in space and time, (15). Similar schemes reported in [9] and [10], which consist of one nonlinear functional transformation followed by a linear canonical transformation, appear to be much more involved than the scheme we have developed.

Under lossless ($\nu = 0$) and local ($g = 0$) approximations (32a) to (32c) can be solved analytically via Laplace transformation as

$$W(t) = 1 \tag{35a}$$

$$\phi_1(t) = \cosh\beta t + [(B-\Gamma)/\beta]\sinh\beta t, \tag{35b}$$

$$\phi_2(t) = (-i\Gamma/\beta)\sinh\beta t, \tag{35c}$$

where

$$\beta \equiv [B(2\Gamma - B)]^{1/2}. \tag{36}$$

Solutions (35a) to (35c) are identical to that calculated by Herrmann [10] utilizing a hypothetical equation of motion. The unknown parameter q used by Herrmann [10] characterizing the local cubic nonlinearity is therefore identified in this paper as $q = 4\pi/9$. We must emphasize here that due to the smallness of the exchange effect parameter B defined in (31a) is a very small number in comparison to other field sources for ordinary values of delay times. In fact under normal echoing conditions we can set B equal to zero in (32b) and (32c) without appreciably affecting the solutions of $\phi_1(t)$ and $\phi_2(t)$. Solution (35a) to (35c) can hardly represent the real solution, since it predicts an echo gain which can be possibly visualized only at extraordinarily large delay times. However, at such large delay time values the spin relaxation effect expressed in (34) will reduce the gain to an insignificant value, since the microwave magnetization relaxes to zero.

Equations (32a) to (32c) can be solved numerically using the fourth order Runge–Kutta method. For 100 steps this method provides solutions with errors less than one part in ten thousand as corresponding solutions are compared with their analytic counterparts, (35a) to (35c). We take the following physical parameters for YIG crystal:

$$4\pi M_s = 1750 \text{ Oe},$$

$$\Lambda = 4.13\times10^{-11} \text{ cm}^2,$$

$$\lambda = 5.4\times10^3 \text{ s}^{-1}.$$

The above corresponds to an exchange energy of 0.4×10^{-6} erg/cm and a line width of $\Delta H = 1/3$ Oe at 9 GHz. The carrier frequency, f, will be assumed to be 1 GHz ($= \gamma H_{dc}$) unless otherwise specified. The cross dimensions of the sample are fixed to be

$$a = b = 1 \text{ mm}.$$

Since parameter B is insignificant in affecting the solutions, the effects of the sample's cross dimensions can be visualized through changing the field gradient values G as indicated in (31b). Finally, in order to convert the excitation rf-field amplitude, $|A_o|$, into power we will assume the sample to have an active region of volume ≈ 100 mm^3.

Results

Fig. 2 shows a typical plot of the echo gain characteristics as a function of delay time τ. The field gradient used in the calculation was $G = 1000$ Oe/cm, and the pump

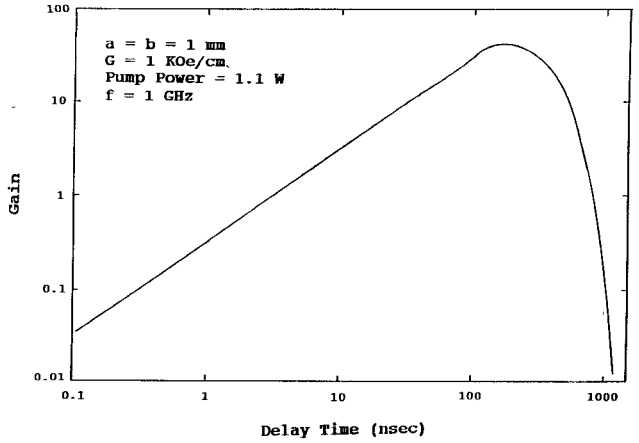

Fig. 2. Echo gain as a function of delay time.

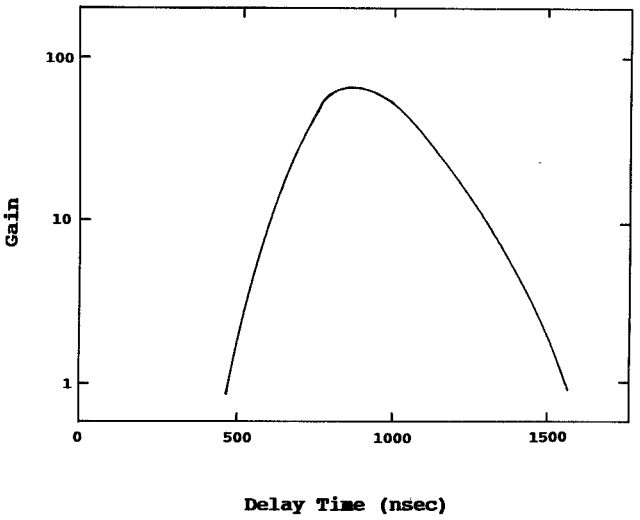

Fig. 3. Experimental echo gain as a function of delay time for pump power = 2 W (cited from [2]).

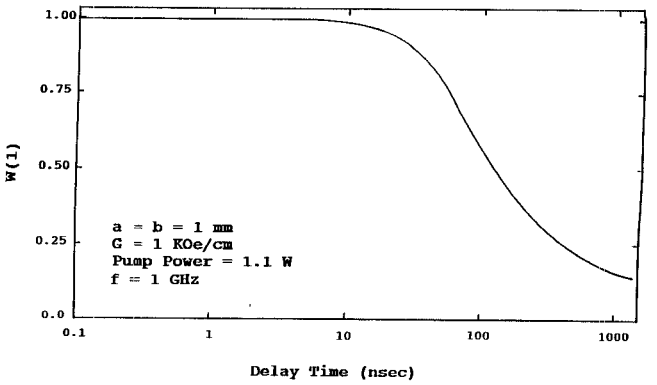

Fig. 4. $W(1)$ as a function of τ.

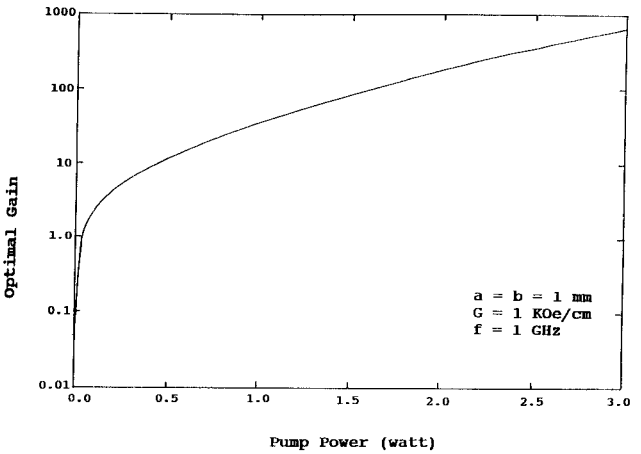

Fig. 5. Optimal gain as a function of pump power.

field $A = 0.3$ ($|A_o| = 16.8$ Oe). This corresponds to a cw excitation power of the pump signal as 1.1 W. Fig. 3 shows the plot of experimental echo gain data as a function of delay time measured by Kaplan *et al.* at X-band for YIG crystal samples [2]. The applied pump power in Fig. 3 was 2 W. It is seen that Fig. 2 compares very well with Fig. 3 quantitatively and qualitatively with respect to τ. The echo amplitude increases with increasing pulse separation τ, reaching a maximum at some optimum value of τ, and decreasing again for large τ. Echo gain with the above feature is unique to ferrimagnetic echoes. For other types of echoes, say nuclear spin echoes, maximum gain occurs right after the application of the pump signals, and the initial growth of the gain with τ is lacking [8]. Fig. 4 shows the corresponding plot of $W(1)$ as a function of delay time τ. When multiplied by $\exp(-\nu\tau)$, Fig. 4 represents the amplitude of the magnetic moment excited by the pump pulse at the instant that echo signal occurs. Under local and lossless approximations as assumed in other calculations $W(1)$ assumes a constant value equal to unity as indicated in (35a). In this calculation in which non-vanishing g and vanishing ν are used, $W(1)$ can be solved analytically as

$$W(1) = \left[1 + (\Gamma/g)\ln(1+g^2)\right]^{-1/2}, \qquad (37)$$

which reduces to zero logarithmically for large values of τ. Therefore, it is the non-locality g that reduces $W(1)$ to zero at large τ-values. The effect of long range dipole-dipole interaction is to reduce the internal rf magnetic field to zero and hence the rf magnetic moment. This means that although the rf magnetic moments are in phase upon the application of the excitation pulse the dipole-dipole interaction will tend to uncorrelate the rf moments and eventually reduce the moment to zero after sufficient elapsed time. Hence, the moment reduces to zero even if the relaxation time is infinite. Of course, with finite relaxation times as we have assumed in our calculation it can only increase the rate of rf magnetic moment reduction as shown in Fig. 4. Once the moment is reduced to zero, the gain will be small. Our calculations demonstrate this effect, as shown in Figs. 2 and 4.

The effect of pump power on the magnitude of maximum gain is shown in Fig. 5, where the field gradient was assumed to be $G = 1000$ Oe/cm. We find that the gain is small for initial power values. It increases rapidly until a

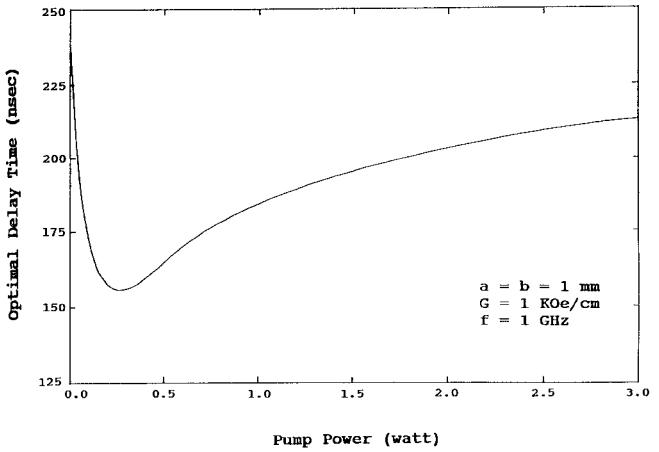

Fig. 6. Optimal delay time as a function of pump power.

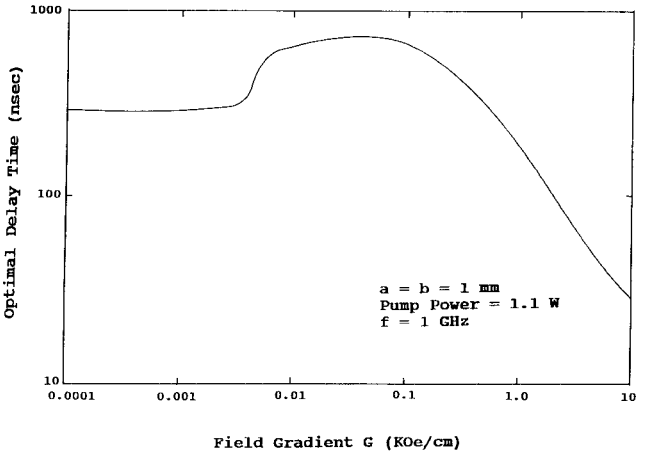

Fig. 8. Optimal delay time as a function of field gradient.

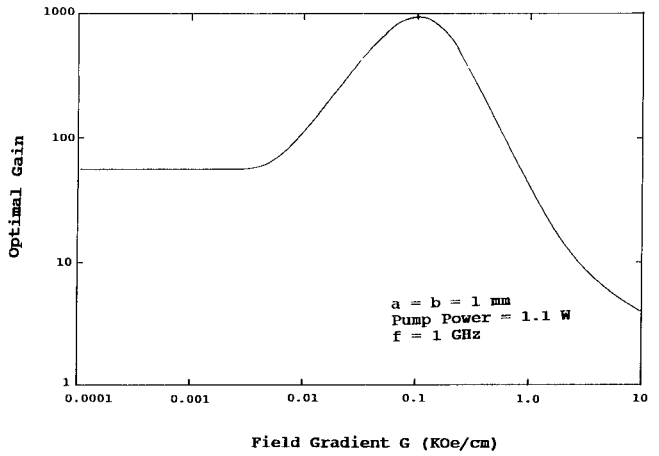

Fig. 7. Optimal gain as a function of field gradient.

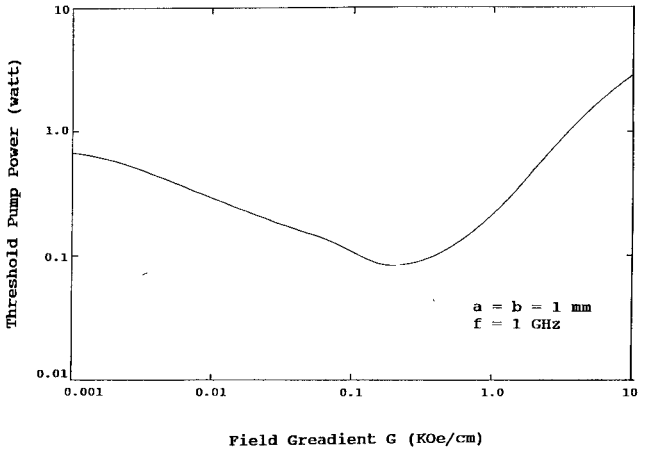

Fig. 9. Threshold pump power as a function of field gradient.

threshold power is reached beyond which the gain presumes large values. The corresponding plot of optimal delay time (at which maximum gain occurs) versus pump power is shown in Fig. 6. For low power amplification the gain is small and the optimal delay time decreases with increasing pump power. For high power amplification the gain becomes large and the optimal delay time, instead, increases with increasing pump power. A threshold power can be therefore defined at which the optimal delay time is a minimum. Therefore, in order to obtain significant echo amplification the pump power must exceed certain threshold value for a given echo experiment.

When the input power of the pump pulse is fixed ($=1.1$ W), the effect of field gradient on the optimal echo gain is shown in Fig. 7. It is seen that the gain takes a maximum value at a field gradient approximately equal to 100 Oe/cm. The gain becomes constant (≈ 55) in the limit of very low field gradient and it goes to zero when the field gradient is high. The corresponding plot of the optimal delay time versus field gradient is shown in Fig. 8. It is seen that optimal delay time presumes maximum value at the field gradient at which maximum gain occurs. For low field gradient the optimal delay is constant (275 ns), while it decreases monotonically at large values of field gradient. Fig. 9 shows the plot of threshold pump power as a function of field gradient. It is seen that minimum power is required in echo amplification when the field gradient takes a value close to 100 Oe/cm.

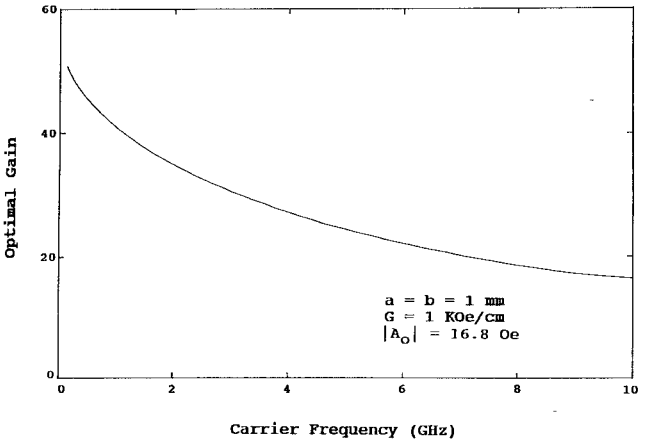

Fig. 10. Optimal gain as a function of carrier frequency.

Figs. 10 and 11 show the effects of carrier frequency on optimal echo gain and delay time, respectively. We have used $G = 1000$ Oe/cm and $A = 0.3$ in calculating these

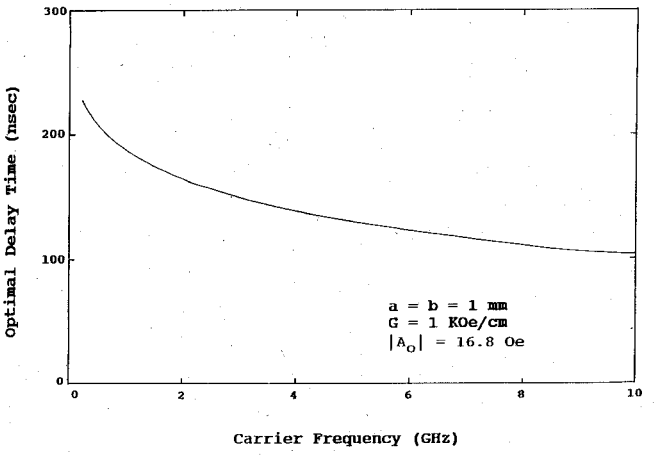

Fig. 11. Optimal delay time as a function of carrier frequency.

two figures. The carrier frequency will influence the magnitude of spin relaxation time, and, hence, we expect the gain to decrease with increasing frequency, as shown in Fig. 10. Fig. 11 also shows that the optimal delay time decreases with increasing carrier frequency. Finally, we wish to point out here that Figs. 2 and 4 to 10 will change inappreciably if the exchange constant $\lambda = 0$ was used in the calculations. Therefore, exchange field could be ignored in considering the amplification of ferrimagnetic echoes.

Discussion and Conclusion

Based upon the order of approximation of previous work we have introduced three extra terms in the nonlinear equation of motion to account for magnetization relaxation, external rf-field coupling, and long range dipole-dipole interaction effects on the excitation and amplification of echoes. These effects were purposely introduced by us in order to provide a realistic mean of relaxing the magnetization to zero after the removal of the excitation pulse. Echoes are produced through the nonlinearity of the equation of motion caused by the excessive amplitude of the pump signal. We have shown in this paper that delay of amplified echoes to an optimum time is a direct consequence of the nonlocal interaction imposed in the formulation. This is contrasted with the previous theory [10] which assumed the exchange effect to be the dominant field in amplifying an echo, see (35c) and (36). The present theory also provides ways for evaluating directly the input pump power through the coupling of the external rf field. The sample's cross sectional dimensions have been proven important with regard to echo gain. This calculation predicts optimal design parameters for the performance of AFEDs including optimal field gradient, threshold pump power, and carrier frequency effects, and hence, should provide future guidance into the design of optimal AFED's.

References

[1] D. E. Kaplan, *Phys. Rev. Lett.*, vol. 14, p. 254, 1965.
[2] D. E. Kaplan, R. M. Hill, and G. F. Herrmann, *J. Appl. Phys.*, vol. 40, p. 1164, 1969.
[3] F. Bucholtz and D. C. Webb, *J. Appl. Phys.*, vol. 54, p. 5331, 1983.
[4] ____, in *Proc. 1982 Ultrasonic Symposium*, IEEE Publ. 82CH1823-4, p. 547.
[5] D. E. Kaplan, *Phys. Lett.*, vol. 53A, p. 149, 1975.
[6] F. Bucholtz, D. C. Webb, and C. W. Young, *J. Appl. Phys.*, vol. 56, p. 1859, 1984.
[7] F. Bucholtz and D. C. Webb, in *Proc. 1983 Ultrasonic Symposium*, IEEE Publ. 83CH1947-1, p. 221.
[8] A. Korpel and M. Chatterjee, *Proc. IEEE*, vol. 69, p. 1539, 1981.
[9] G. F. Herrmann, D. E. Kaplan, and R. M. Hill, *Phys. Rev.*, vol. 181, p. 829, 1969.
[10] G. F. Herrmann, R. M. Hill, and D. E. Kaplan, *Phys. Rev. B*, vol. 2, p. 2587 1970.
[11] H. How and C. Vittoria, *Phys. Rev. Lett.*, vol. 66, no. 12, p. 1626, 1991.
[12] M. Sparks, *Phys. Rev. B*, vol. 1, p. 3831, 1970.
[13] ____, *Ferromagnetic Relaxation Theory*. New York: McGraw-Hill, 1964, p. 69.
[14] H. Suhl, *J. Phys. Chem. Solids*, vol. 1, p. 299, 1957.
[15] B. Lax and K. J. Button, *Microwave Ferrites and Ferrimagnetics*. New York: McGraw-Hill, 1962, sec. 4.3.

Hoton How received the B.S. degree in physics from National Tsing Hua University, Taiwan, in 1976, and the Sc.D. degree in Materials Sciences and Engineering from Massachusetts Institute of Technology, Cambridge, MA, in 1987.

Currently he is working as the Senior Scientist in the Microwave Materials Group in the Electrical and Computer Engineering Department at Northeastern University. His research interests include nonlinear ferrimagnetic phenomena, artificial materials, antennas, superconductivities, EMP effects, and various microwave/superconducting device work. Mr. How has published more than 30 refereed papers and has two U.S. patents in application.

C. Vittoria (S'62–M'80–SM'83–F'90), photograph and biography not available at the time of publication.

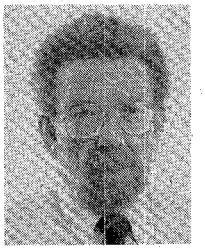

Glen E. Everett (A'89) received the B.A. degree in physics from the University of Utah, Salt Lake City, in 1956, and the S.M. and Ph.D. degrees in physics from the University of Chicago, Chicago, IL, in 1957 and 1962, respectively.

He joined the University of California, Riverside in 1961 where he is a Professor of Physics. In 1963, he began research collaboration at the Naval Ordinance Laboratory, Corona, in the areas of microwave assisted superconducting tunneling and in antiferromagnetic resonance. He has been associated with the Naval Weapons Center, China Lake, since 1971. His research interests include magnetic anisotropy and resonance, spin wave resonance, dietectric constant measurements, and microwave filter theory.